*Materials Transactions*, Vol. 44, No. 2 (2003) pp. 290 to 297


# Effect of Under Bump Metallurgy and Reflows on Shear Strength and Microstructure of Joint between Cu Substrate and Sn–36Pb–2Ag Solder Alloy

Seung Wook Yoon[1], Jong Hoon Kim[2], Sang Won Jeong[2] and Hyuck Mo Lee[2,*]

[1]*Advanced Package Development Support, Institute of Microelectronics (IME), 11 Science Park Road, Science Part II, 117685 Singapore*
[2]*Department of Materials Science and Engineering, Korea Advanced Institute of Science and Technology, Kusung-Dong 373-1, Yusung-Gu, Taejon, 305-701 Korea*

The interfacial reaction between Sn–36Pb–2Ag (numbers are all in mass% unless specified otherwise) solder balls and Ni, Ag and Ni/Ag electroplated on a Cu substrate was investigated and the joint bonding strength was measured using a ball shear tester. The intermetallic $Ag_3Sn$ was observed at the interface of the Cu/Ag/solder joint and $Ni_3Sn_4$ was found at the Cu/Ni/solder joint. In the case of Cu/Ni/Ag substrate, the layer sequence was observed to be Cu/Ni/$Ni_3Sn_4$/$Ag_3Sn$/solder. The Ag layer was completely consumed by formation of $Ag_3Sn$ but the Ni layer remained. Environmental tests showed that the Cu/Ni/Ag substrate retained better solder joint reliability than either Ni or Ag single plated Cu substrate. Two types of reflow profiles were tested and the specimen reflowed by a higher temperature profile showed a higher solder joint strength. Solder joint strength and microstructural change were observed with several reflow cycles in considering the real board mounting conditions. There was significant evolution of solder and joint microstructures with reflow cycles and it explained well the change of solder joint strength.

(Received August 5, 2002; Accepted November 28, 2002)

***Keywords:*** *tin–lead–silver solder, under bump metallurgy, interfacial reaction, solder joint strength, joint microstructure, interfacial intermetallic compound*

## 1. Introduction

Considerable attention has been paid to the development of new packaging technologies aimed at reliable joining technologies for interconnections as device chips become denser and smaller. Concurrently with these emerging packaging technologies, new boundary conditions are foreseen which require stronger solder joints between the Cu substrate and solder alloys.[1)] The reliability of soldered devices is related to wettability of the solder to the substrate and to the microstructural stability of the joint during the soldering operation and/or in use. The microstructure of the joint is related with the interfacial reaction between solder and substrate, thereby the reliability of the solder joint is strongly affected by the type and the extent of the interfacial reaction between solder and substrate. Accordingly, the interfacial reaction between solder and substrate is increasingly important and a deeper understanding of the interfacial reaction is necessary.[2,3)]

During the soldering process, the intermetallic compound (IMC, hereafter) forms at the interface between solder and substrate. The initial formation of the IMC at the interface means a good metallurgical bonding. However, excessive growth of an IMC can strongly affect the subsequent solderability.[4,5)] Generally the solder joints experience at least three reflow cycles on mounting. First is when the solder ball is attached on the solder ball bonding pad. Second is the attachment on the printed circuit board (PCB) substrate and the third is another PCB side attachment of the package in the case of the double side surface mounting. Repair or rework process is carried out if necessary, thereby the solder joints experience four reflow cycles. There is a great possibility of change in interfacial microstructures during these reflow cycles. Furthermore, during aging and field service the IMCs grow, thereby changing the interfacial microstructure and the strength of the solder joint. Actually, thermal fatigue due to temperature fluctuations either from internally generated heating or from the external operating environment is a common solder joint failure mode in electronic assemblies.[6)] These problems become more serious in using small sized solder balls and solder ball bonding pads that are now widely used in many packaging applications such as BGA (Ball Grid Array), CSP (Chip Scale Package) and WLP (Wafer Level Package). In addition to minimizing package dimension, the use of solder balls as the interconnection between the semiconductor package and the PCB or printed wire board (PWB) is beneficial in decreasing the interconnection length and thus improving electrical performance.

In this work, three kinds of UBM (Under Bump Metallurgy), Ni, Ag and Ni/Ag prepared by an electroplating process were used on a Cu substrate. We examined their effect on the solder joint strength and the microstructural change of the interface between the substrate and the Sn–36Pb–2Ag solder. Mechanical properties and microstructures were investigated with environmental tests, aging time, reflow temperature profiles and number of reflow cycles.

## 2. Experimental Procedures

The LF(Lead Frame)-CSP[7,8)] using a ball grid array and Cu lead frame was used in this study. The Sn–36Pb–2Ag solder ball (Tanaka Denshi Kogyo, Japan) with an average diameter of 0.45 mm was used. The Cu lead frame was made from C7025 (Olin, USA) and the chemical composition is shown in Table 1. The ball land diameter of the Cu substrate was 0.36 mm. The Ni, Ag and Ni/Ag layers were prepared by electroplating on Cu substrate as UBM of LF-CSP. The thickness of the electroplated layers of Ni, Ag and Ni/Ag was

*Corresponding author. E-mail: hmlee@kaist.ac.kr

Table 1 Chemical compositions of Cu alloy, C7025.

| Nominal composition (mass%) | Ni | Si | Mg | Cu |
|---|---|---|---|---|
| C7025 Cu alloy | 3.00 | 0.65 | 0.15 | 96.20 |

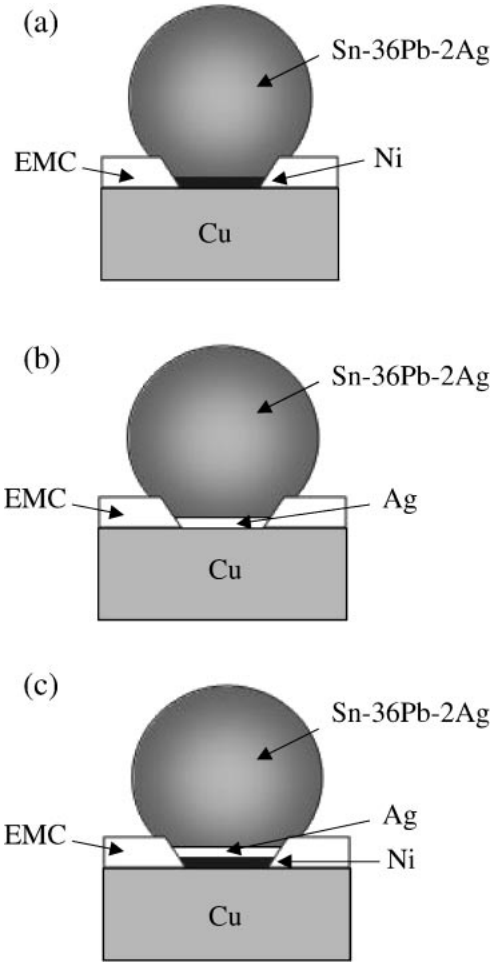


Fig. 1 Schematic diagrams of UBM system; (a) Cu/Ni/Sn36Pb2Ag solder bump, (b) Cu/Ag/Sn36Pb2Ag solder bump and (c) Cu/Ni/Ag/Sn36Pb2Ag solder bump. EMC is epoxy molding compound.

Table 2 Temperature profiles of reflow furnace.

| | $T_{max}$ (°C) | holding time above 183°C (s) | holding time above 200°C (s) |
|---|---|---|---|
| Profile 1 | 235 | 140 | 80 |
| Profile 2 | 220 | 60 | 35 |

measured by SFT3200 (XRF coating thickness gauge) and it was $2 \pm 0.25\,\mu m$ for each Ni and Ag layer. Figure 1 shows the schematic UBM systems used in this study. Soldering was performed in an infrared reflow furnace and two different types of temperature or reflow profiles were used. These profiles are listed in Table 2 and plotted in Fig. 2. The maximum temperatures in profiles 1 and 2 were 235°C and 220°C respectively. The melting point of the Sn–36Pb–2Ag solder alloy is 179°C.

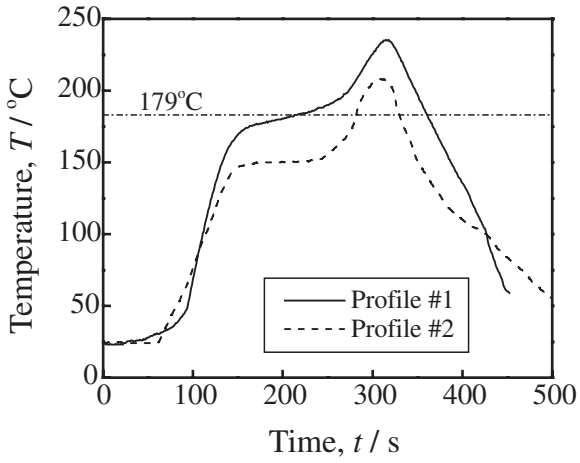


Fig. 2 Temperature profiles of reflow furnace; profile 1 is represented by solid line and profile 2 is represented by dotted line. The melting point of Sn–36Pb–2Ag is 179°C.

Two severe environmental tests were carried out to investigate the package level reliability; temperature cycle test (−65°C–150°C up to 500 cycles) and pressure-cooker test (0.2 MPa (2 atm), 121°C, 100% Relative Humidity up to 240 h). Both are accelerated environmental tests that are normally practiced in the packaging assembly factory. Then the solder ball shear test followed to measure the solder joint strength using a Dage 2400 ball shear tester.

Each solder joint was vertically cut and cold-mounted. They were then mechanically polished with a 1 μm diamond automatic polisher. In order to observe clearly the morphology of the IMC at the interface, the solder matrix was removed by etching in a $HNO_3$ solution for several seconds. The interface was examined using a back-scattered (BS) scanning electron microscope (SEM) operated at 25 kV. The composition profiles were measured by a Noran energy dispersive X-ray (EDX) detector in point mode. X-ray diffraction (XRD) analysis was also performed to identify the phases.

To investigate the solid state growth kinetics of the IMC, the joint specimens attached with the solder ball were reflowed two times by profile 1. These specimens were then annealed at 125°C and 150°C for up to 1000 h. The solder ball shear test was then performed to measure the solder joint strength using a Dage 2400 ball shear tester.

## 3. Results

### 3.1 Solder joint characteristics with UBM systems

Microstructures and EDX analyses of an interfacial IMC layer formed when the Sn–36Pb–2Ag solder ball was soldered on Cu/Ag by reflow of profile 1 are shown in Figs. 3(a,b) respectively. EDX results, Fig. 3(b), show that the IMC formed is $Ag_3Sn$. The morphology was rough and round. The original Ag layer was almost completely consumed to form the $Ag_3Sn$ IMC. These observations are in accordance with previous findings.[9,10] In the case of soldering Sn–36Pb–2Ag on Cu/Ni, a different type of IMC was formed at the interface as seen in Fig. 3(c). It was identified as $Ni_3Sn_4$ according to the EDX of Fig. 3(d) and the XRD of Fig. 3(e). The solder

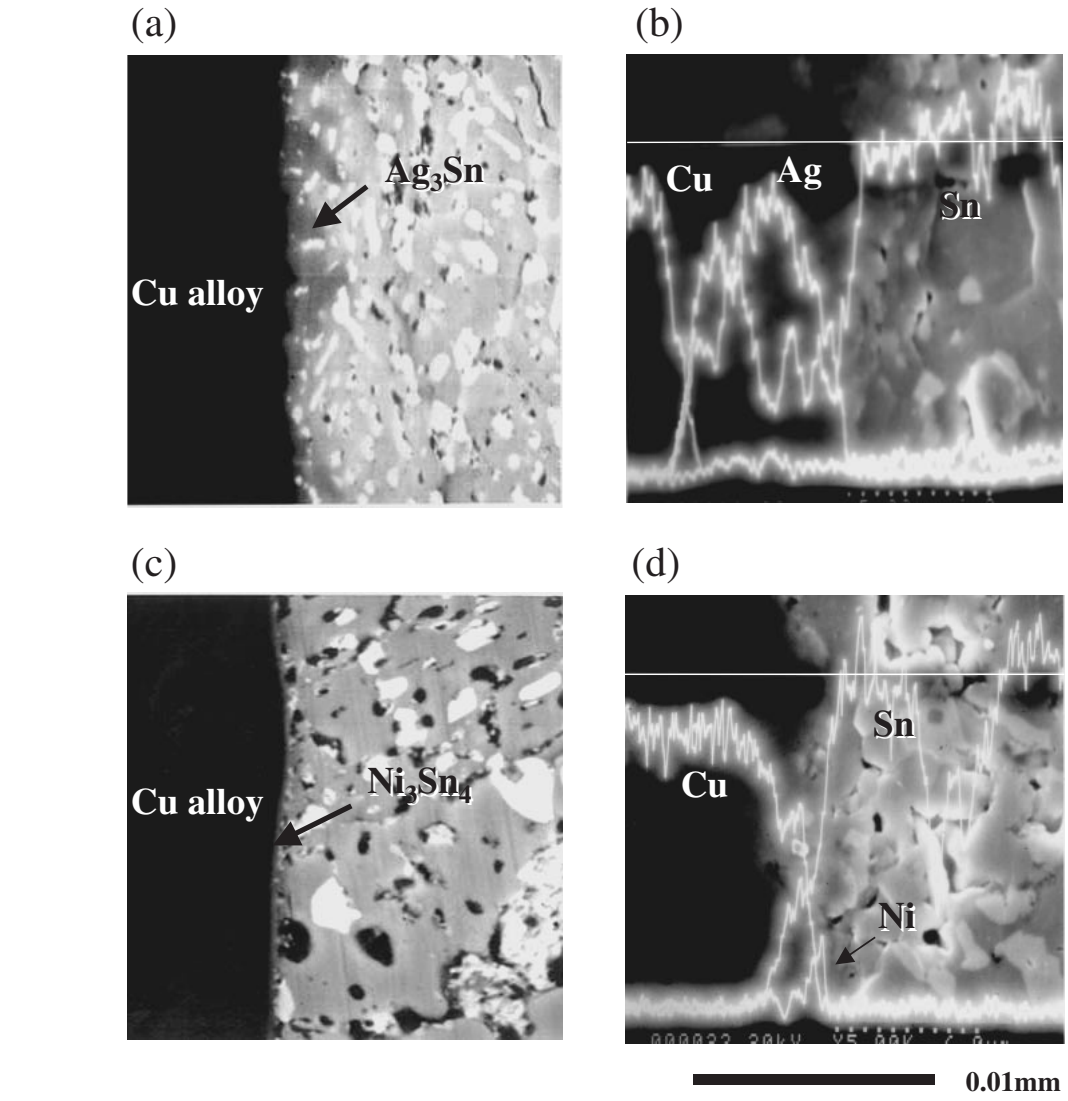


Fig. 3 Joint interface between solder and Cu/Ag; (a) SEM micrograph and (b) EDX analysis. Joint interface between solder and Cu/Ni; (c) SEM micrograph, (d) EDX analysis and (e) XRD analysis. Soldering was made by reflow of profile 1.

ball was removed by etching in $HNO_3$. Thus the $Ni_3Sn_4$ IMC particles were clearly identified although some of the Sn and Pb elements still remained. According to the Sn–Ni phase diagram,[11] there is a potential for additional IMC phases of $Ni_3Sn$ and $Ni_3Sn_2$ to appear. The appearance of the $Ni_3Sn_4$ phase in the soldering reaction has been successfully explained through the activation energy value.[12] In the case of the joint between Sn–36Pb–2Ag and Cu/Ni/Ag substrate, a layer sequence of Cu–Ni–$Ni_3Sn_4$–$Ag_3Sn$-solder was obtained although the relevant interfacial microstructure will be shown in Section 3.2. The original Ag layer was all consumed by the formation of $Ag_3Sn$. Most of the Ni layer

remained and a $Ni_3Sn_4$ layer formed.

Figure 4 shows the change of solder ball shear strength after each environmental test. There were up to 500 temperature cycles in the former test and the time duration was up to 240 h in the latter. Initially, the Cu/Ni/Ag/solder bump had a medium joint strength with the solder ball between those of Cu/Ag/solder and Cu/Ni/solder. The Cu/Ni/solder bump had a higher joint strength, which implies that the dissolution of Ni into the solder is more effective in solid solution strengthening compared with the dissolution of Ag in the Cu/Ag/solder bump. After 240 h of pressure-cooker testing, the Cu/Ni/Ag/solder bump system showed higher reliability compared with Cu/Ag/solder and Cu/Ni/solder. Even in the temperature cycle test, a similar behavior in the joint strength was observed and it was found that the Cu/Ni/Ag/solder bump was superior after 200 and 500 cycles. The Cu/Ni/Ag substrate retained higher joint shear strength than the others after both tests, which implies that this UBM is more reliable. Therefore, the Cu/Ni/Ag UBM was selected and further experiments were carried out with this UBM.

### 3.2 Solder joint characteristics with number of reflow cycles

The effect of reflow profiles and number of reflow cycles on microstructural evolution and solder joint strength was studied for the solder joints on Cu/Ni/Ag UBM. Four reflow cycles were applied to the solder joint with different soldering temperature profiles 1 and 2 of Fig. 2. Profile 1 is the normal soldering temperature profile having a maximum temperature of 235°C while a slightly lower maximum temperature of 220°C is used in profile 2. Figure 5 shows the variation of the solder ball shear strength with the number of reflow cycles. For reflow profile 1, the joint strength increased after the second reflow and decreased after the third and fourth reflow cycles. The shear strength was always higher than in the initial state of the first reflow. In contrast to reflow profile 1, there was a sudden drop in the solder joint strength after the second reflow at profile 2 and it increased after the third and fourth reflow cycles. Except for the first reflow, the solder joint strength reflowed with profile 1 maintained a higher value than reflow profile 2.

The interfacial microstructure was investigated with the BS mode of SEM. Figure 6 is for the joint reflowed at temperature profile 1 with up to four cycles. Figure 6(a) shows the microstructure after the first reflow. Pb-rich areas are bright and Sn-rich areas are dark inside the solder, a continuous $Ag_3Sn$ IMC layer was observed at the interface. Inside several Pb-rich grains the secondary precipitation of Sn particles was observed, which takes place due to the solubility difference of Sn on cooling in the Pb matrix.[13] They are called Pb-rich pockets or islands.[14] According to Fig. 6(b) that shows the interface after the second reflow, the interfacial $Ag_3Sn$ layer disappeared and the solder micro-

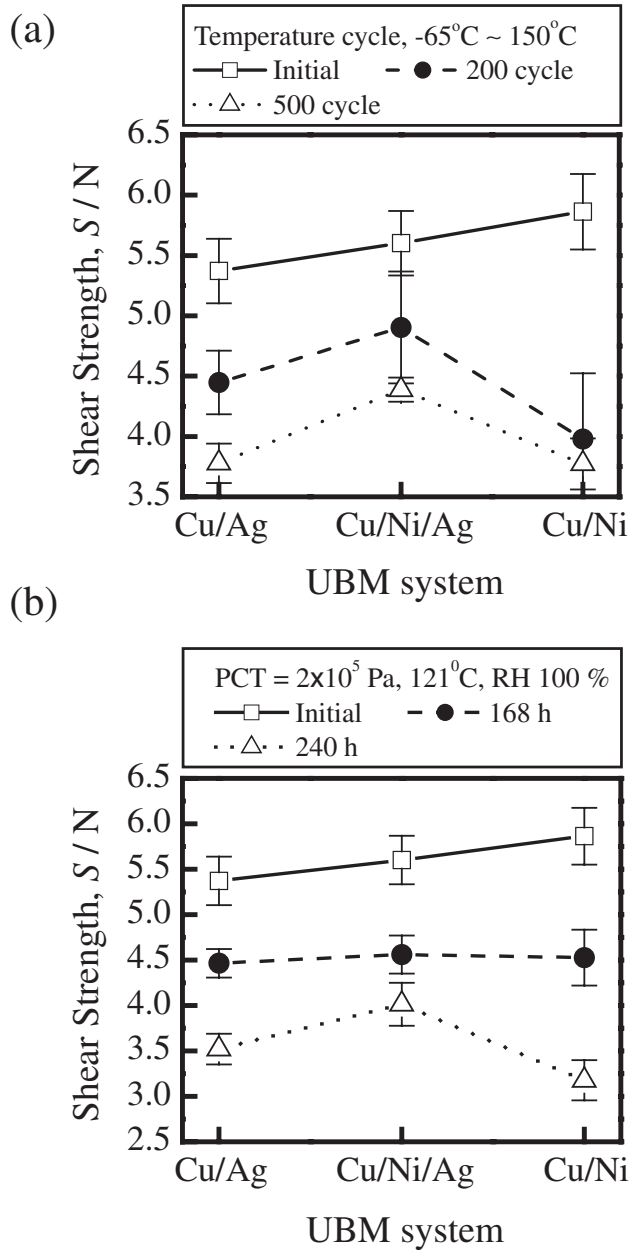


Fig. 4 Variation of solder ball joint strength on Cu/UBM after (a) temperature cycle test and (b) pressure-cooker test.

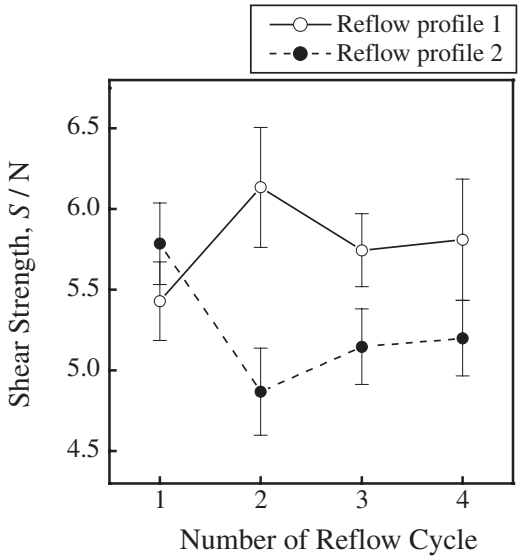


Fig. 5 Variation of solder ball joint strength on Cu/Ni/Ag with number of reflow cycles. Both profiles were used.

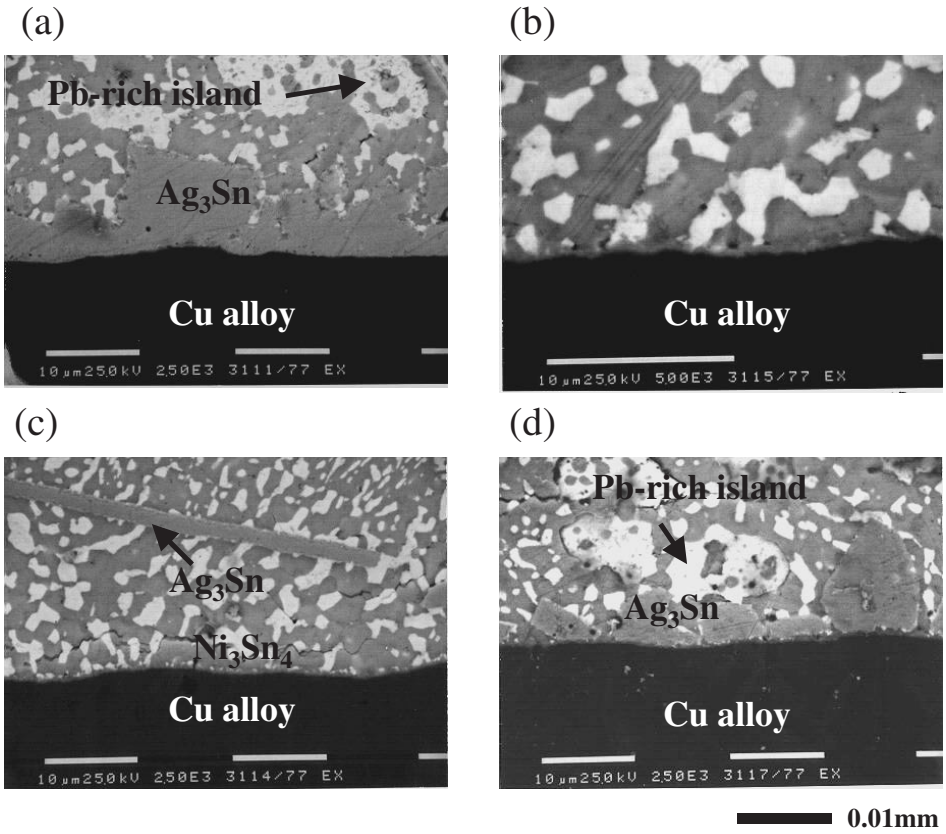


Fig. 6 SEM micrographs of solder joint interface on Cu/Ni/Ag reflowed at temperature profile 1; (a) first, (b) second, (c) third and (d) fourth reflow.

structure became homogeneous without Pb-rich pockets. After the third reflow, the $Ni_3Sn_4$ layer was found and the isolated rod-type $Ag_3Sn$ particles formed inside the solder as shown in Fig. 6(c). Its length was in the range of 20–50 μm. It also had a homogenous solder microstructure. After the fourth reflow in Fig. 6(d), the isolated $Ag_3Sn$ particles precipitated at the interface and several Pb-rich pockets were found inside the solder.

The presence of the interfacial $Ni_3Sn_4$ layer was sometimes hard to identify due to thinness but it formed in all the cases. The interface was line scanned after the third and fourth reflows and the results are shown in Fig. 7. The sharp peak of Ni shows that the Ni layer remained even after the third and fourth reflows and it played a major role as a diffusion barrier against the copper substrate.

Figure 8 shows the influence of reflow numbers on the joint

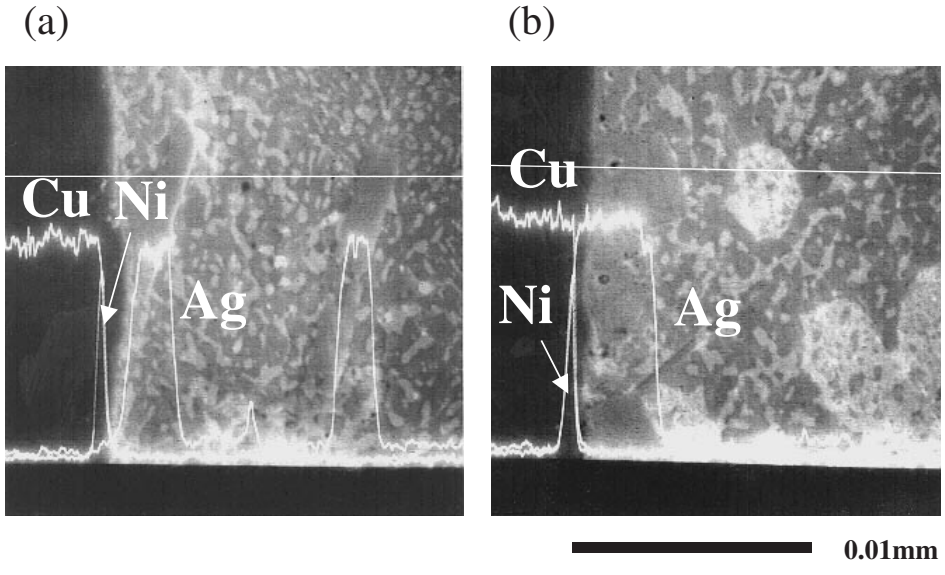


Fig. 7 EDX line scanning of the solder joint interface on Cu/Ni/Ag after (a) third and (b) fourth reflow. Profile 1 was used.

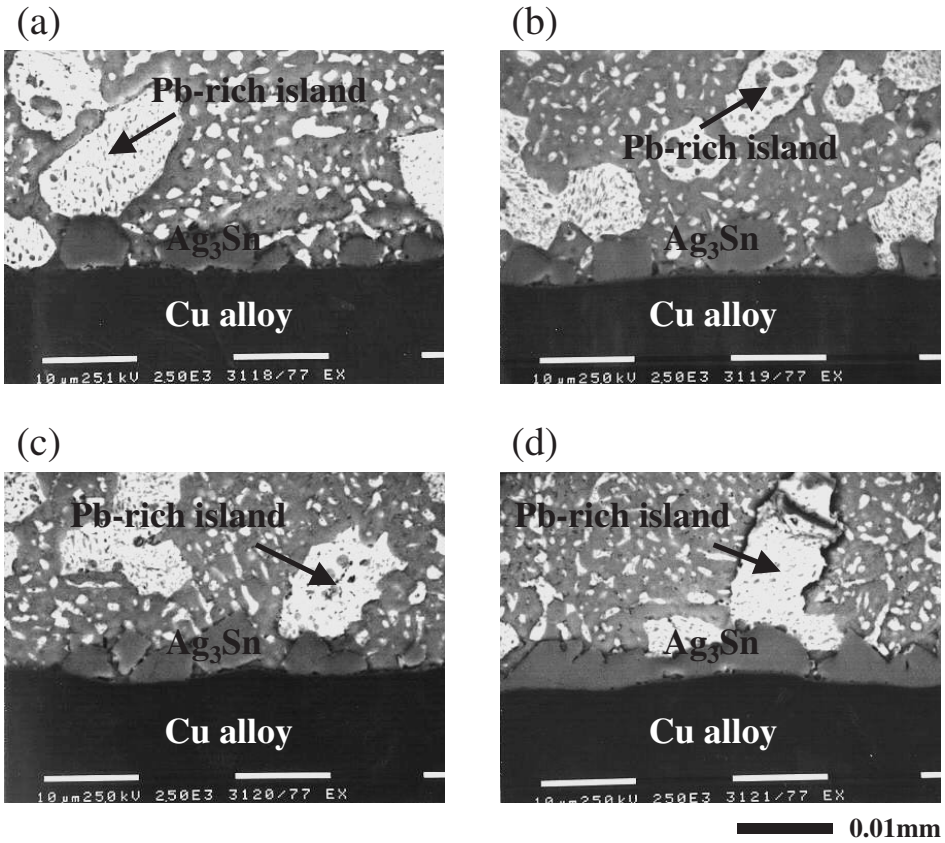


Fig. 8 SEM micrographs of the solder joint interface on Cu/Ni/Ag reflowed at temperature profile 2; (a) first, (b) second, (c) third and (d) fourth reflow.

interfacial microstructure when temperature profile 2 was used. As the number of reflows increased, the $Ag_3Sn$ grains precipitated at the interface and their size increased probably by coarsening and eventually they formed a continuous IMC layer, shown in Fig. 8(d). The sudden decrease of the solder joint strength after the second reflow can be related to the coarsened morphology of the interfacial $Ag_3Sn$ particles. Coarsening of the interfacial $Ag_3Sn$ particles causes the exhaustion of both Ag in solder and UBM, thereby degrading the strength of the solder itself and the solder joint.

### 3.3 Solid state growth kinetics of IMC

Figure 9 shows the variation of solder joint strength with annealing time at 125°C and 150°C. The strength decreased with the increase of annealing time and temperature. Figure 10 illustrates the change of IMC thickness with time and a parabolic relationship was obtained between thickness and time. The growth kinetics of $Ni_3Sn_4$ seems to be controlled by solid state diffusion. Compared with the data from Blair *et al.*,[1] the Ni/Ag substrate showed slighter larger IMC thickness but the slope was almost the same as that of Ni or Ni/Sn–10Pb.

The SEM fractographs of the joint specimens that were reflowed or heat-treated at 125°C and 150°C for 1000 h are shown in Fig. 11. Figure 11(a) shows the reflowed specimen imaged in a normal mode and Fig. 11(b) is imaged in the BS mode. The planar surface was composed of Sn and Pb, which shows that the fracture occurred inside the solder, not through the IMC layer. When the specimens were heat-treated, the surface showed a less ductile fracture mode as seen in Figs. 11(c,d). Nonetheless the fracture occurred in the solder even after high temperature annealing. This suggests that the solder joint strength is greater than the strength of the solder itself.

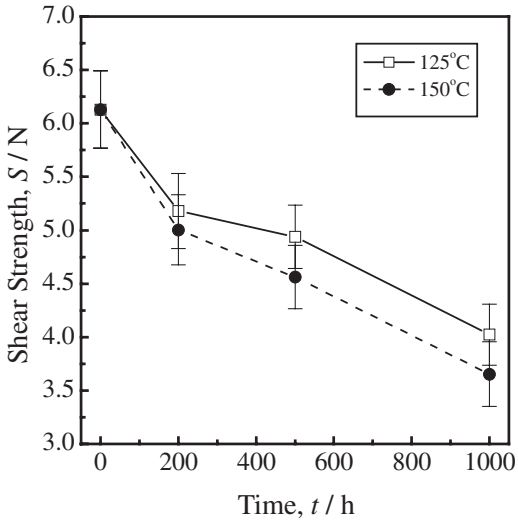


Fig. 9 Variation of the solder ball joint strength on Cu/Ni/Ag with aging time at 125°C and 150°C. Joint was reflowed two times by profile 1.

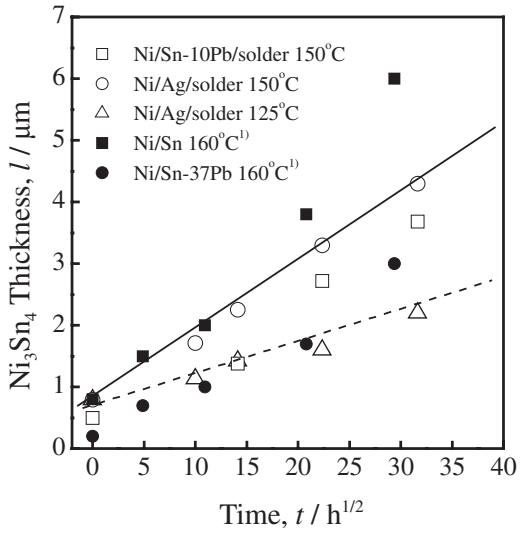


Fig. 10 Growth kinetics of $Ni_3Sn_4$ in Ni/(UBM)/solder joint. Data shown by filled symbols are from Ref. 1) and data denoted by empty symbols are from this study.

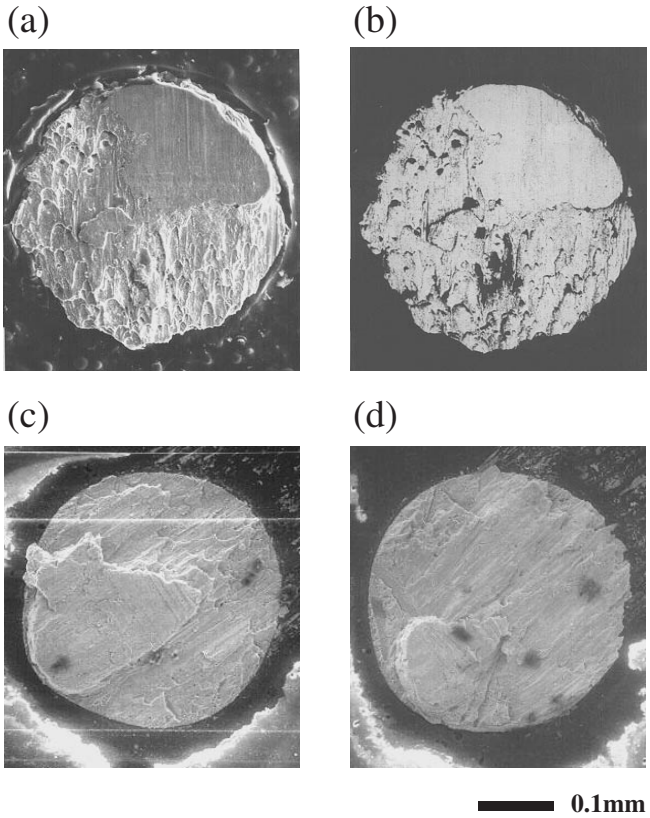


Fig. 11 SEM fractographs of the joint reflowed by profile 1; (a) normal image and (b) back-scattered image. (c) is for the joint aged at 125°C for 1000 h and (d) is for aging at 150°C for 1000 h.

## 4. Discussion

There was a significant change in microstructures of solder and joint after reflow of both profiles 1 and 2. It must be related with dissolution and precipitation during reflow. Especially for profile 1 with a higher maximum temperature, the interfacial $Ag_3Sn$ layer that formed after the first reflow by reaction of Sn in solder and Ag in UBM dissolved after the second reflow, and the $Ag_3Sn$ particles precipitated inside the solder bulk after the third reflow. It is highly likely that the excessive amount of Ag in UBM was dissolved into the solder during several reflows, then it reacted with Sn and precipitated as a stable form of $Ag_3Sn$ in the bulk solder. They precipitated again at the interface after the fourth reflow. The solder microstructure changed, too, during reflows. According to Figs. 6(a,d) where the $Ag_3Sn$ layer formed at the interface, the Pb-rich pockets were found. As shown in Figs. 6(b,c), however, there was no interfacial $Ag_3Sn$ and a homogeneous microstructure was obtained without Pb-rich islands.

For profile 2 the $Ag_3Sn$ IMC was always observed at the interface and the Pb-rich islands precipitated irrespective of number of reflow cycles. The Pb-rich islands are generally observed at off-eutectic solder compositions such as 50Sn–50Pb (high Pb-content solder).[14] This implies that some amount of Sn in the solder was consumed to form the $Ag_3Sn$ layer at the interface. The original solder composition was then changed to lower the Sn content and to increase Ag, thereby the cooling path changed as to precipitate the Pb-rich phase first during cooling after reflow. The Pb-rich phase precipitated as a primary phase from the liquid. In this way the Pb-rich islands formed inside the solder matrix. According to the phase equilibria calculations by Thermo-Calc,[15] the $Ag_3Sn$ phase is a primary phase for the original Sn–36Pb–2Ag system as shown in Fig. 12.

Figure 13 shows the variation of the shear strength as a function of IMC thickness for the joint reflowed by profile 1. Overall, it showed a tendency to decrease with an increase in thickness of the interfacial IMC. This can be explained well if the fracture occurred through the IMC layer at the interface. However, the fracture occurred inside the solder ball as shown in Figs. 10(a,b). As a result, the change of joint strength is more complex and may not be explained by the change of the interfacial IMC thickness alone. During several reflow cycles, the dissolution of Ag in the solder and UBM and Ni in UBM took place and it might have changed the

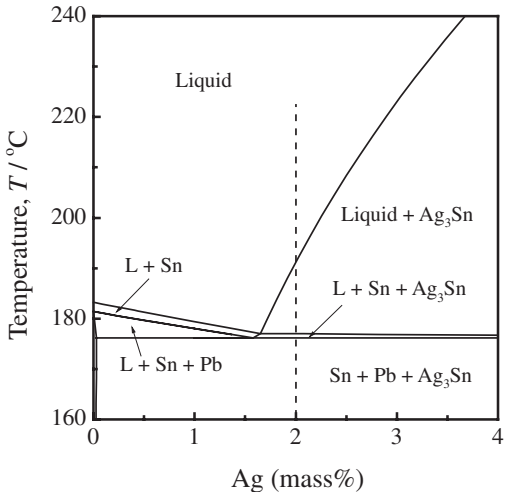


Fig. 12 Calculated phase diagram of the Sn–36Pb–Ag ternary system.

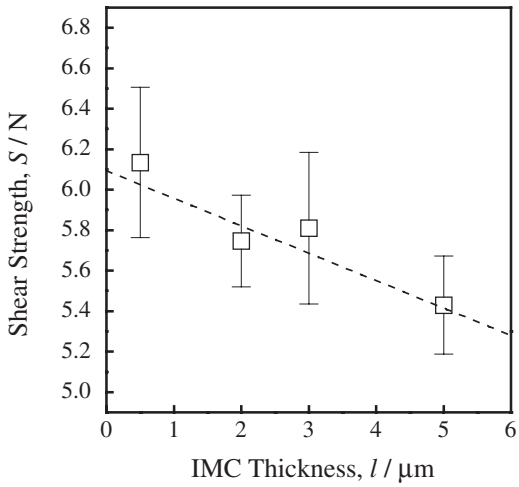


Fig. 13 Result of ball shear test as a function of interfacial IMC thickness for the joint of Cu/Ni/Ag/Sn–36Pb–2Ag reflowed by profile 1.

hardness and strength of the solder itself by changing the composition of the solder ball. It has been demonstrated by Choi *et al.*[16] that the joint strength is closely related with the microstructure and the hardness value of the bulk solder when the fracture occurs in a ductile mode. The inherent grain growth and coarsening of the solder matrix may be another clue for the decrease of solder joint strength with annealing time and temperature.

## 5. Summary

Among three kinds of UBM, the Cu/Ni/Ag substrate retained the highest joint shear strength after both environmental tests. The variation of the solder ball shear strength with the number of reflow cycles was measured using two kinds of temperature profiles. We suggest the change of shear strength for profile 1 can be explained by the compositional change of the solder and thus the change of hardness and strength of the solder itself. We propose the change of shear strength for profile 2 to be due to the coarsened morphology of the interfacial IMC particles. The change of microstructure of solder and joint was observed with the number of reflow cycles and it was explained by dissolution, solidification and phase equilibria. The fracture occurred inside the solder, not through the IMC layer.

## Acknowledgments

This study has been supported by the CEPM (Center for Electronic Packaging Materials) of the KOSEF (Korea Science and Engineering Foundation).

## REFERENCES

1) H. D. Blair, T.-Y. Pan and J. M. Nicholson: 48th Electronic Components and Technology Conference, (Seattle, 1998) pp. 259–267.
2) H. M. Lee, S. W. Yoon and B.-J. Lee: J. Electron. Mater. **27** (1998) 1161–1166.
3) D. R. Frear, W. B. Jones and K. R. Kinsman: *Solder Mechanics*, (TMS, Warrendale, 1991) pp. 29–104.
4) J. H. Lau: *Solder Joint Reliability*, (Van Nostrand Reinhold, New York, 1991) pp. 406–454.
5) P. L. Tu, Y. C. Chan and J. K. L. Lai: IEEE CPMT Part B **20** (1997) 87–93.
6) D. Solomon: J. Electron. Packaging **114** (1992) 161–168.
7) S. W. Yoon, J. T. Moon, S. H. Hong. Y. H. Choi and C. J. Park: Semicon-Korea 1999, (Seoul, 1999) pp. 171–179.
8) J. T. Moon, S. H. Hong, S. W. Yoon, C. J. Park, Y. H. Choi, J. M. Kim, J. H. Lee, J. R. Kim and Y. H. Koh: 49th Electronic Components and Technology Conference, (San Diego, 1999) pp. 1235–1240.
9) P. J. Kay and C. A. MacKay: Trans. Inst. Met. Finish **54** (1976) 68–74.
10) X. H. Wand and H. Conard: Scr. Metall. **30** (1994) 725–730.
11) T. B. Massalski: *Binary Alloy Phase Diagram*, 2nd ed., (ASM International, Materials Park, 1991) pp. 2863–2864.
12) W. K. Choi and H. M. Lee: Scr. Mater. **46** (2002) 777–781.
13) D. R. Frear, J. B. Posthill and J. W. Morris, Jr.: Metall. Trans. **20A** (1989) 1325–1333.
14) D. R. Frear, S. N. Burchett, H. S. Morgan and J. H. Lau: *The Mechanics of Solder Alloy Interconnects*, (Van Nostrand Reinhold, New York, 1994) pp. 12–14.
15) B. Sundman, B. Jansson and J. O. Andersson: CALPHAD **9** (1985) 153–190.
16) W. K. Choi, J. H. Kim, S. W. Jeong and H. M. Lee: J. Mater. Res. **17** (2002) 43–51.